Atmospheric Environment 96 (2014) 175–185

Contents lists available at ScienceDirect

Atmospheric Environment

journal homepage: www.elsevier.com/locate/atmosenv

Intercomparison of planetary boundary layer parameterization and its impacts on surface ozone concentration in the WRF/Chem model for a case study in Houston/Texas

G.C. Cuchiara [a,*], X. Li [a], J. Carvalho [b], B. Rappenglück [a]

[a] University of Houston, Department of Earth and Atmospheric Science, 4800 Calhoun Rd, Houston, TX 77204-5007, United States
[b] Universidade Federal de Pelotas, Faculdade de Meteorologia, Pelotas, RS, Brazil

HIGHLIGHTS

- We presented a sensitivity analysis study of WRF/Chem employing different PBL schemes.
- We performed a case study during VME/TRAMP project over Houston TX.
- YSU scheme represents better the vertical mixing of O_3 precursors over this region.

ARTICLE INFO

Article history:
Received 5 February 2014
Received in revised form
2 July 2014
Accepted 3 July 2014
Available online 3 July 2014

Keywords:
Planetary boundary layer
Atmospheric modeling
WRF/Chem
PBL parameterization

ABSTRACT

With over 6 million inhabitants the Houston metropolitan area is the fourth-largest in the United States. Ozone concentration in this southeast Texas region frequently exceeds the National Ambient Air Quality Standard (NAAQS). For this reason our study employed the Weather Research and Forecasting model with Chemistry (WRF/Chem) to quantify meteorological prediction differences produced by four widely used PBL schemes and analyzed its impact on ozone predictions. The model results were compared to observational data in order to identify one superior PBL scheme better suited for the area. The four PBL schemes include two first-order closure schemes, the Yonsei University (YSU) and the Asymmetric Convective Model version 2 (ACM2); as well as two turbulent kinetic energy closure schemes, the Mellor–Yamada–Janjic (MYJ) and Quasi-Normal Scale Elimination (QNSE). Four 24 h forecasts were performed, one for each PBL scheme. Simulated vertical profiles for temperature, potential temperature, relative humidity, water vapor mixing ratio, and the *u*–*v* components of the wind were compared to measurements collected during the Second Texas Air Quality Study (TexAQS-II) Radical and Aerosol Measurements Project (TRAMP) experiment in summer 2006. Simulated ozone was compared against TRAMP data, and air quality stations from Continuous Monitoring Station (CAMS). Also, the evolutions of the PBL height and vertical mixing properties within the PBL for the four simulations were explored. Although the results yielded high correlation coefficients and small biases in almost all meteorological variables, the overall results did not indicate any preferred PBL scheme for the Houston case. However, for ozone prediction the YSU scheme showed greatest agreements with observed values.

© 2014 Elsevier Ltd. All rights reserved.

1. Introduction

Numerical Weather Predictions (NWP) and air quality models (AQM) are widely used as a basis for decision-making processes, not only to predict severe weather phenomena but also to develop ambient pollutant regulations. Nowadays, NWP models operate with horizontal resolution varying in a range of 1–100 km. However, there are still relevant scales of atmospheric motions which are not properly resolved, and these effects must be included in NWP models to reasonably predict the atmospheric states. In the atmosphere, turbulent motions play an important role in the sub-grid scale, and can considerably alter the vertical mixing within the planetary boundary layer (PBL). In most regional scale NWP models, the PBL parameterizations are responsible to represent the

* Corresponding author.
E-mail address: gustavo.cuchiara@gmail.com (G.C. Cuchiara).

http://dx.doi.org/10.1016/j.atmosenv.2014.07.013
1352-2310/© 2014 Elsevier Ltd. All rights reserved.

impact of sub-grid scale turbulent motions on larger grid-scale variables, such as potential temperature, water vapor mixing ratio, and wind. As the PBL can present a variety of distinct characteristics, many different formulations exist with the objective to represent the real state of the atmosphere. Furthermore, these impacts of different parameterizations are not only confined to meteorological variables in NWP models, but also must be well represented in air-quality models (AQM) to properly simulate the concentration of trace gases.

There are two distinctive approaches to parameterize the vertical fluxes in NWP models utilizing different closure schemes. Closure schemes are used to obtain turbulent fluxes from mean atmospheric variables at grid cell level (Holt and Raman, 1988). These closure schemes are indispensable since that the number of unknown variables in the set of equations for turbulent flow is larger than the number of equations after applying Reynolds averaging to the fundamental equations. There are two common approaches for turbulence closure: local and non-local closure (Stull, 1988). The local closure scheme estimates the turbulent fluxes at each model grid cell by using mean atmospheric variables and/or their gradient at a grid cell and its immediate neighboring cells. Thus it assumes that turbulence is analogous to molecular diffusion. However, this technique represents an oversimplification of the convective boundary layer where large eddies play an important role in vertical transport. On the other hand, non-local closures schemes assume that the unknown quantity at one model grid cell is parameterized by values of known quantities at grid cells of various levels. This assumes that turbulence is a superposition of eddies of different scales, each of which transports fluid like an advection process (Stull, 1988).

Sub-grid scale fluxes can affect thermodynamic and dynamic properties in the whole troposphere through vertical diffusion of heat, moisture and momentum (Skamarock et al., 2008). Many different PBL parameterization have been suggested with various treatments of specific PBL properties and processes (e.g. stability, vertical transfer of momentum, heat and water vapor by turbulence, and the absorption and emission of radiation at the surface and within the atmosphere) as well as how these properties and processes are represented. The technique of non-local closure has been applied to problems of vertical mixing in convective boundary layers (e.g. Stull and Driedonks, 1987; Blackadar, 1978). A few recent studies examined the sensitivity of the Weather Research and Forecasting (WRF) (Skamarock et al., 2008) model predictions to PBL schemes (Jankov et al., 2007; Borge et al., 2008; Gilliam and Pleim, 2010; Mohan and Bhati, 2011; Xie et al., 2013; Yver et al., 2013; Hu et al., 2013; Wilmot et al., 2014). The performance of different PBL schemes vary depending on the PBL conditions, e.g. nonlocal PBL schemes were reported represent better vertical transport by eddies, hence they present better performance than local PBL schemes in the daytime convective boundary layer. Ha and Mahrt (2001) illustrated that vertical mixing in the residual layer was an important source of model uncertainties. Vertical resolution was shown to affect the modeled vertical mixing strength. Sensitivity simulations with different treatments of vertical mixing (i.e. different stability functions and asymptotic lengths) in the residual layer were conducted to identify the proper treatment. This investigation was extended by Hu et al. (2010) who focused on the sensitivity of the WRF model for simulating the daytime convective boundary layer. Hu et al. (2010) evaluated three PBL schemes in the WRF model for the Houston–Galveston area. Yerramilli et al. (2010) evaluated the sensitivity of the PBL and land surface physics in ozone predictions with the Weather Research and Forecasting model with Chemistry (WRF/Chem) model over the Central Gulf Coast Region. The authors suggested the combination of the Yonsei University PBL scheme with the Noah land surface scheme for the best model representation, mainly when compared with observed vertical profiles data derived from radiosondes. Also, they highlighted that the main differences between experiments are due to distinct PBL parameterization of turbulent exchange coefficients. Tang et al. (2011) analyzed the uncertainties in the formulation of vertical diffusion schemes in associated model parameters and their effect on ozone prediction using the Community Multi-scale Air Quality (CMAQ) model. For some high ozone episodes the authors found that the choice of vertical diffusion scheme can affect the 8-h ozone sensitivity towards NO_x by approximately 20%, and by 5–10% due to the uncertainty in dry deposition velocities. More recently, Kolling et al. (2013) evaluated the Asymmetric Convective Model, version 2, (ACM2) with two distinctive NWP in Southeast Texas. The authors showed that the ACM2 scheme accurately simulate the morning growth, maximum height, and evening decay of the daytime PBL in this region.

The Houston metropolitan area is the fourth-largest metropolitan area in the United States, with over 6 million inhabitants. Located in southeast Texas this region frequently exceeds the National Ambient Air Quality Standard (NAAQS) for ozone (U.S. EPA, 2008a). Thus, a realistic simulation of the planetary boundary layer structure and its evolution is critical for modeling of meteorology and air quality in this region. Indeed, poor accuracy in the simulated physical properties often leads to degraded meteorological and air quality prognostic skills.

In this study, we employed the WRF/Chem model to quantify meteorological prediction differences produced by four widely used PBL schemes and compared the results to observational data obtained on a day in the 2006 TexAQS-II radical and aerosol measurement project (TRAMP) campaign, when temporally highly resolved boundary layer data was collected in the Vertical Mixing Experiment (VME) which formed part of TRAMP. The methodology of the sensitive analysis used in this study is described in section two. After validating the meteorological variables, a sensitivity analysis of the surface ozone was performed within the chemistry package of the WRF model, which is presented in the third section. Finally, conclusions are compiled in the last section.

2. Methodology

The first part (chapter 3.1 and 3.2) of the study address the implementation of the WRF model and comparing the results against a unique and comprehensive data set during the VME subproject of the TRAMP study, focusing on the vertical mixing simulated by the model. The meteorological observations include frequent rawinsonde soundings, ozonesondes, tethersonde, surface and aircraft measurements. The third and fourth parts (chapter 3.3 and 3.4) of the study show a sensitivity analysis of surface ozone to different PBL schemes. The results from WRF/Chem are compared to surface stations from both, the VME experiment and the Continuous Ambient Monitoring Site (CAMS) network in Houston. The sensitivity of PBL schemes are analyzed for one day, October 5, 2006 during the Vertical Mixing Experiment (VME), a sub-project of the larger TRAMP study. A full description of the TRAMP study is provided by Lefer and Rappenglueck, 2010. The Advanced Research Weather Research and Forecast (ARW-WRF) model version 3.5 with chemistry was used (Grell et al., 2005), and conducted with three model domains with one-way nesting technique. Please see Table 1 for information about model configuration. For further information about model configuration and parameterization of PBL in WRF please see Supplementary material (SM). Also, in SM there is a brief description of synoptic conditions on October 5, 2006 (Fig. S2).

Table 1
Simulation characteristics.

Domain number	1	2	3
Period	6 October 2006		
Initial condition meteorology	NCEP Eta (40 km)		
Initial condition chemistry	MOZART-4 (2.8 × 2.8°; 28 vertical levels)		
Vertical level	42	42	42
Horizontal grid (*x*,*y*)	157 × 127	100 × 100	151 × 136
Horizontal resolution	36 km	12 km	4 km
Time step	180 s	120 s	30 s
Microphysics	WSM5		
Advection scheme	5ª horizontal/3ª vertical		
Long wave radiation scheme	RRTM		
Short wave radiation scheme	Dudhia		
Land surface	NOAH		
Chemistry mechanism	RADM2		
Dry deposition	Wesley, 1989		
Biogenic emissions	MEGAN		
Anthropogenic emissions	NEI2005		
Photolysis	Madronich, 1987		
Aerosols option	MADE/SORGAM		

Rawinsonde soundings were released from the University of Houston (UH) main campus (29.74 N; 95.34 W; 11 m) above ground level (agl) approximately 5 km to the southeast of downtown Houston. The atmospheric sounding profiles provide meteorological variables such as temperature, potential temperature, mixing ratio, and *u*−*v* components of the wind. On this day rawinsondes were launched at 0500, 1000, 1600, and 1900 Central Daylight Time (CDT).

Vaisala, Inc.'s DigiCora III Tethersonde System was used for the experiments. All the soundings were taken consecutively in profile mode using the same TTS-111 tethersonde. Tethersonde measurements were taken at varying intervals on seventeen periods in this day, 0834, 0910, 0932, 1102, 1115, 1130, 1139, 1148, 1204, 1300, 1309, 1321, 1346, 1434, 1803, 1816, and 1831 CDT. The observations were made from a few meters above the ground up to 300 m agl, allowing the comparison between observed and simulated data in the lowermost first model levels (12, 46, 97, 180, 268, 360, 443 m agl). The data was averaged for every 10 m above the ground level. Additional information about rawinsonde and tethersonde data and analysis can be found in Rappenglück et al. (2008) and Day et al. (2010).

Two stations obtained meteorological variables on the UH main campus. The meteorological variables measured were temperature, relative humidity, and *uv*-components of the wind. The first station was located at the roof of north Moody Tower residence hall, which is located 65 m agl (29.7176 N, 95.3414 W). The second station was located at the balloon launching site on the UH campus (29.7421 N, 95.3395 W).

The aircraft measurements were collected on board of the Baylor University (BU) Aztec aircraft. The aircraft performed 5 spirals over the UH main campus collecting vertical profiles of temperature, relative humidity, *u* and *v* components of the wind. The chemistry variables collected were Carbon Monoxide (CO), Formaldehyde (HCHO), Sulfur Dioxide (SO_2) and Ozone (O_3). Description of the instrument payload is given in Olaguer et al. (2009).

The CAMS network in Houston was used to validate the model against observed O_3 and NO_x surface concentration, more specifically the CAMS stations included Houston East (C1), Aldine (C8), Bayland Park (C53), Clinton (C403), Northwest Harris County (C26), and Texas City (C620).

With regard to rawinsondes statistical analysis included observed and modeled vertical profiles of temperature, potential temperature, water vapor mixing ratio, and *u*−*v* components of the wind. Also, statistical analysis was applied to evaluate the relationship between temperature, relative humidity, *u*−*v* components of the wind, and ozone simulated by WRF/Chem and observed at the Ground Trailer and atop the Moody Tower. Statistical Analysis was also performed to the CAMS ozone and nitrogen oxides data. The calculated parameters included the Pearson correlation coefficient (*R*) to determine strength of linear association between the forecasts and observations, the root mean square error (RMSE), to describe the magnitude of the difference between predicted and observed values, and the multiplicative bias (BIAS), which is the ratio of the means of the forecasts and the observations.

3. Results and discussion

3.1. Sensitive analysis with PBL and its impact on vertical mixing processes

One of the vital parameters that has a critical impact on air quality is the planetary boundary layer height. The PBL determines the mixing in the lower atmosphere and defines the atmosphere diffusivity. Since the determination procedure for the PBL height is a characteristic feature of each PBL scheme, and WRF/Chem does not have a minimum PBL height value imposed at night, we compare the PBL heights of the four experiments. The simulated nocturnal PBL height ranges from 16 to 80 m agl from ACM2, YSU, and MYJ (Fig. 1a), with YSU being the scheme that calculated the lowest PBL height during almost all nighttime. The simulated nocturnal PBL height from QNSE ranges from 160 to 400 m agl. However, during the daytime the development of PBL is a consequence of the convective turbulence, which generates huge differences in the PBL height according to the different treatments. The PBL schemes based on eddy-diffusivity (MYJ and QNSE) present less PBL increase during the day when compared to PBL schemes based on bulk Richardson number (YSU and ACM2). Fig. 1a shows that PBL height varies from 1500 to 2400 m. The YSU and ACM2 PBL scheme produced the highest PBL height during daytime, and also the lowest vertical mixing during nighttime. A subjective way to estimate the PBL height from observation based on Rappenglück et al. (2008) was used in this work. The result of these observations can be visualized as black dots in Fig. 1a, and the PBL heights estimated were 400, 500, 700, 1600, 1400 m agl at 05, 07, 10, 16, and 19 CDT, respectively. We estimate the uncertainty of the PBL height to be on the order of ±50 m. Although this subjective estimation of the PBL height does not yield very precise values, the calculated PBL height values by the different PBL schemes is also subject to uncertainties. Please see SM for further information about how PBL schemes calculate PBL height.

Vertical profiles of ambient temperature (K), potential temperature (K), mixing ratio (g/kg), relative humidity (%), and *u*−*v*

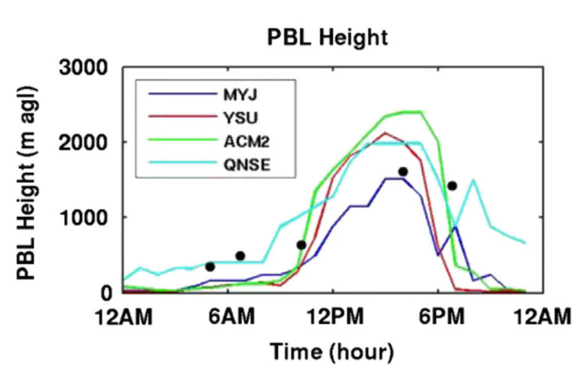

Fig. 1. Planetary boundary layer height time series for October 05, 2006.

components of wind were selected to further explore differences of PBL schemes and their potential impact on vertical mixing. Please see Appendix A for a brief description about weather Fig. 2 shows the observations based on rawinsondes soundings compared against the four experiments calculated by WRF/Chem, from the surface up to 5 km agl. Fig. 3 presents the comparisons between the Tethersonde vertical profiles and model results from the surface to an altitude of 300 m agl.

Fig. 2 shows a comparison between model experiments and rawinsonde data released from UH campus at 05, 10, 16, and 19 CDT. Clearly, the differences between the experiments are more evident during the daytime (16 and 19 CDT), when the PBL exhibits a pronounced diurnal variation, and the different parameterization schemes calculate its evolution distinctly. The model calculates well the temperature vertical profile (Fig. 2a and f), basically at all levels with the exception of the surface, where modeled values are too low at around 05 CDT. The model did not calculate well the inversion layer at 10 CDT (400 m agl in the observations versus 300 m agl in the YSU, MYJ, and ACM2 experiments, and 200 m agl in the QNSE experiment).

Compared to the observations the model simulated lower potential temperatures below 2500 m agl (Fig. 2b and g). In addition, Fig. 2g shows that the potential temperature calculated by the experiments in the layer between 500 and 1500 m agl can reach up to 2 K of difference at 19 CDT. The inconsistency between the θ-profiles of the experiments is presumably due to differences in local and non-local mixing and entrainment formulations. The divergences between the PBL heights and θ-profiles in the TKE closure experiments (Figs. 1a and 2b,g) is because the PBL height is calculated based on the TKE profiles, rather than on the θ-profiles.

Fig. 2c and h presents comparisons between observed and modeled vertical profiles of water vapor mixing ratio. Although the model reasonably calculates the water vapor vertical profile, there are some evident discrepancies between modeled and observed data, mainly at the level of approximately 1500–3900 m agl. Overall, all modeled water vapor mixing ratio values are higher than the observation for most of altitudes. In Addition, larger differences between the experiments were found below 1500 m agl. In particular at 19 CDT, higher potential temperatures calculated from MYJ and QNSE generated drier atmospheric conditions at this level. Conversely, the YSU and ACM2 results display wetter conditions at this level.

For the wind components (Fig. 2d, e, i, j), the biggest discrepancies can be observed near the surface. None of the experiments can reproduce the fluctuations of the u and v wind components in the mixed layer at 16 and 19 CDT. The observations represent an instantaneous value at a given point and thus also reflect an instantaneous turbulent state at this point, which is one of the main differences of the PBL when compared to the free atmosphere. The fluctuation of these values are not averaged out during the observation, while the PBL schemes reflect effects of sub-grid scales turbulent fluxes to mean variables, consequently the model does not represent the observation variability.

Fig. 3 presents data measured by a tethersonde launched at University of Houston main campus. Seventeen tethersonde profiles were obtained on October 5, however only the most representative times are shown in this work. Overall analysis shows that the model calculated reasonably well the first model levels. The water vapor mixing ratio (first column in Fig. 3) presents lower water vapor mixing ratios before 11 CDT and higher water vapor mixing ratios afterwards, i.e. at 11:15, 12:04, 13:46, 14:34, and 18:31 CDT. In addition, the model calculated well the logarithm shape of the wind profile as expected over urban regions (Stull, 1988), with QNSE scheme displaying the lowest wind speed near the surface. The observational wind data shows that wind speeds are low near the ground. In particular nighttime data indicates that there were stable conditions due to small variations in the vertical profile of the wind speed. On the other hand, daytime values show larger oscillation in the vertical profile of the wind speed, which is due to stronger turbulent fluxes.

Table S2 in SM shows the statistical analysis of model results experiments versus observed rawinsonde data. The results for air temperature vertical profiles show high correlation coefficient for all launches (05, 10, 16, and 19 CDT), and small biases. Among the experiments none of them stands out, the differences between R are in the third decimal.

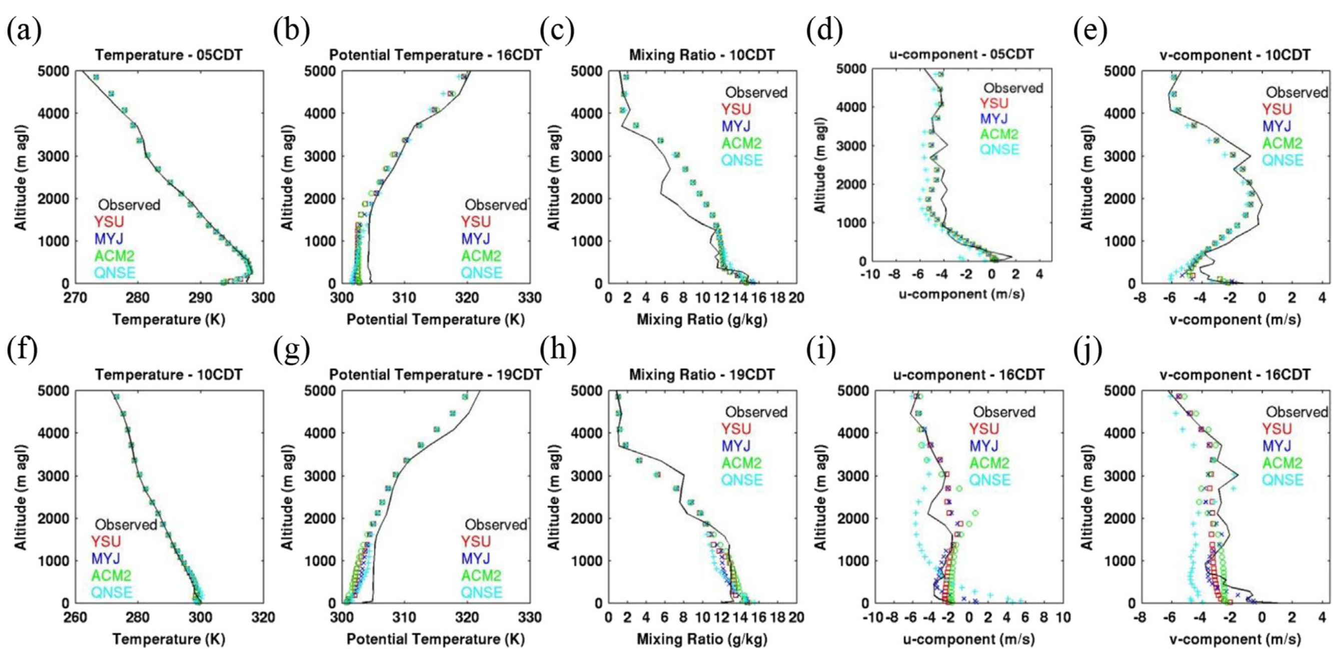

Fig. 2. Rawisondes vertical profiles of air temperature at 5 CDT (a) and 10 CDT (f); potential temperature at 16 CDT (b) and 19 CDT (g), water vapor mixing ratio at 10 CDT (c) and 19 CDT (h), u-component of wind at 5 CDT (d) and 16 CDT (i), and v-component of wind at 10 CDT (e) and 16 CDT (j).

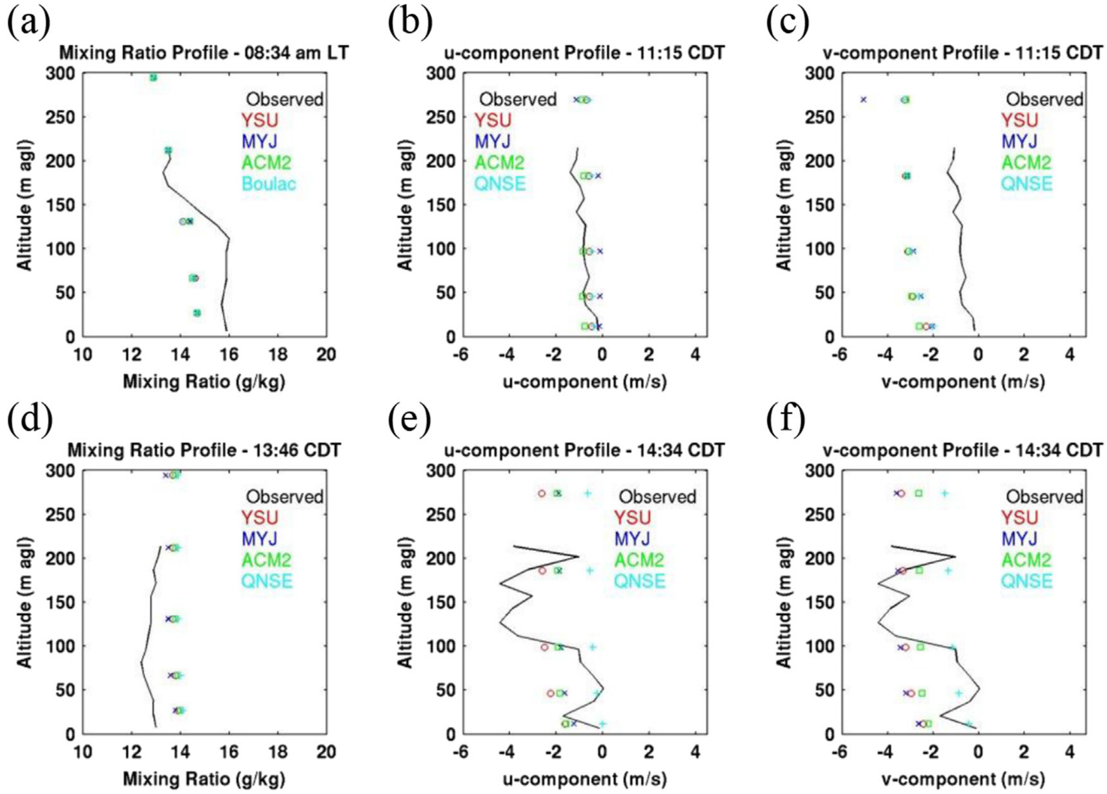

Fig. 3. Tethersonde vertical profiles for water vapor mixing ratio, at 08:34 CDT (a) and 13:46 CDT (d), *u* and *v* component of wind, at 11:15 CDT (b and e), and 14:34 CDT (e and f) on October 5, 2006.

3.2. Diurnal evolution of meteorological variables

Figs. 4 and 5 show the comparisons of PBL with observations from the ground trailer and the Moody Tower, respectively. The temperature time series for the ground trailer station is depicted in Fig. 4a. The model calculates reasonably well the diurnal temperature variations. However, it underestimates the temperature at night. Also, the model calculates well the temperature during major parts of the day, but underestimates the temperature in the afternoon after 01 p.m. This same pattern can be seen for the Moody

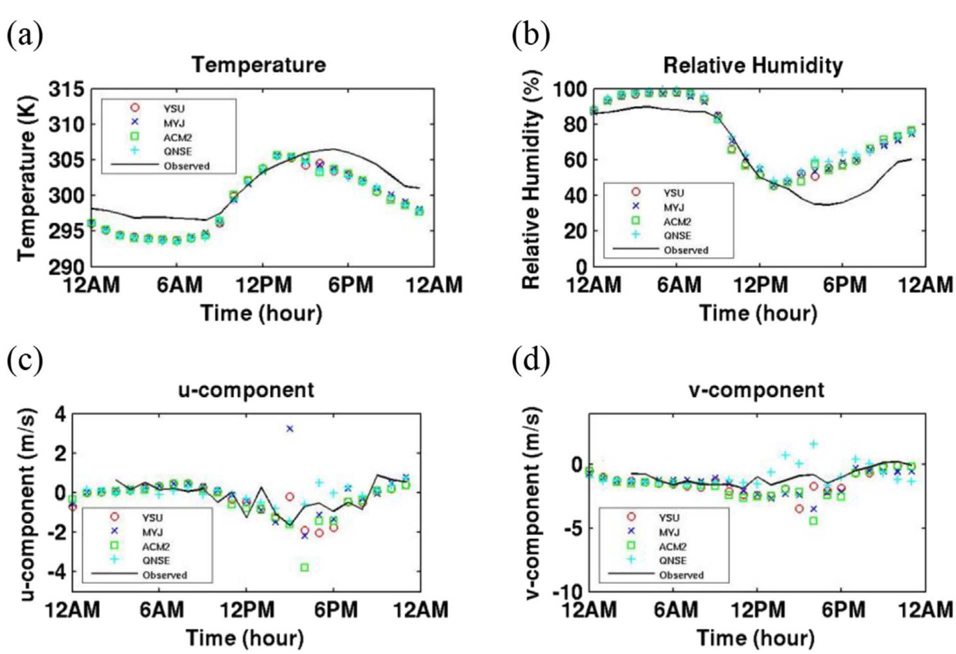

Fig. 4. Ground trailer time series of the observed and simulated surface air temperature (a), relative humidity (b), *u*-component (c), and *v*-component (d) on October 05, 2006.

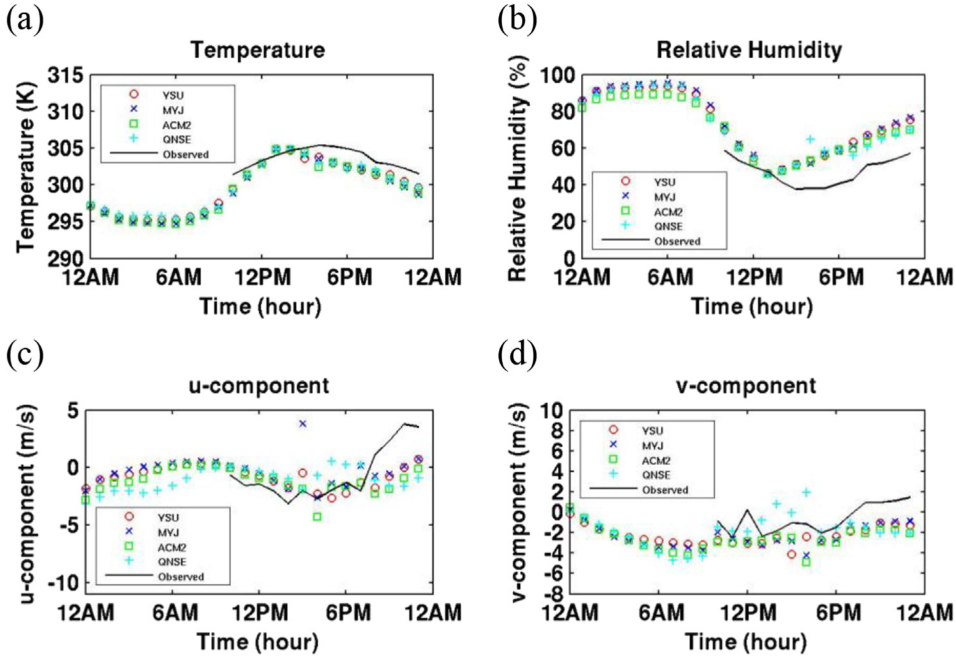

Fig. 5. Moody tower time series of the observed and simulated surface air temperature (a), relative humidity (b), *u*-component (c), and *v*-component (d) on October 05, 2006.

Tower site, where the model underestimates the temperature after 01 p.m. Unfortunately, there is no data available for this site before 10 a.m., so a conclusive statement cannot be made. At both sites the different PBL schemes yield quite similar results for the nocturnal temperature gradient near the surface, underestimating the observed values by 2–3 K. In other words, the four experiments underestimate the surface cooling rate during the PBL collapse, as well as at nighttime.

The relative humidity (Figs. 4b and 5b), which is related to the air temperature, behaves inversely. During nighttime, the model calculates wet biases for relative humidity, but displays good agreement with observations during the daytime growth period of the PBL. On the other hand, the model shows dry biases of relative humidity after 2 p.m. CDT. As mentioned before, it is likely associated with the prediction of higher temperatures at night and lower temperatures during the afternoon. In addition, the poor agreement of relative humidity may be related to the representation of vegetation and soil category data in the WRF/Chem model (Yerramilli et al., 2010). The wet deposition and aqueous chemical processes in the model can be affected by this bias in the modeled humidity data. As a consequence it may result in unrealistic chemical concentrations and deposition rates.

The *u* and *v* component of the wind show some good agreement with the observed values. The biggest difference can be observed in the *v* component and mainly in the comparison with the Moody Tower site. Also, strong winds during the nighttime appear to be a common experience in WRF simulation and many authors experienced this behavior of the model (Misenis et al., 2006; Cheng and Steenburgh 2005; Roux et al., 2009; Yerramilli et al., 2010; Ngan et al., 2013). The discrepancies in the calculation of wind among the experiments can be associated with the differences in the parameterization of the eddy exchange coefficient.

In summary, there is no particularly outstanding algorithm for the meteorological variables. The thermodynamic variables simulated with the four PBL parameterizations are different at daytime, but show converging results at nighttime. We can infer from these results that the representation of the surface variables is still uncertain, even using the most suitable PBL schemes, especially under stable conditions. There is no particularly well-suited algorithm.

3.3. Surface ozone

Simulated O_3 mixing ratio was contrasted with the field observations made at the University of Houston main campus (Ground Trailer and Moody Tower) and observations made by CAMS. Figs. 6 and 7 present the spatial distribution of surface ozone simulated by WRF/Chem and observed by the in-situ stations in the period of October 05 of 2006, at 06 and 15 CDT for the inner domain. Overall, the results show that the model captured the diurnal variations of ozone, with maximum mixing ratios in the afternoon (Fig. 7) and minimum mixing ratios in the morning (06 CDT) (Fig. 6). At night the spatial distribution of ozone is fairly similar in the different experiments. Although the calculated ozone did not reach 0 ppbv as observed by CAMS stations, the lowest values simulated by the model were found in the Houston area. During daytime, the differences between the PBL schemes are clearer, with YSU and MYJ being the schemes which simulated the highest O_3 values.

The O_3 time series of two different altitudes are presented in Fig. 8. The model captured the daytime high O_3 mixing ratios, but overestimated the nighttime O_3 at the ground trailer when compared with the first model level (~11 m agl) (Fig. 8a). However, when the second model level (~60 m agl) was compared with the Moody Tower time series (Fig. 8b), the modeled O_3 values did not reach the highest value of 80 ppbv observed during daytime, and underpredict the O_3 during most of the nighttime. The different model behavior in these two layers may be due to (i) a poor representation of vertical transport of O_3 precursors from the first into second model layer or (ii) an overestimation of NO_x in the second model layer or a combination of both. The scatter plot in Fig. 8 reinforced what was observed in the ground trailer time series, in which the model tends to overestimate the minimum O_3 concentration, and underestimate the maxima O_3 concentration.

It is well-known that single digit nighttime O_3 mixing ratios are attributed to nighttime depletion to the surface through dry

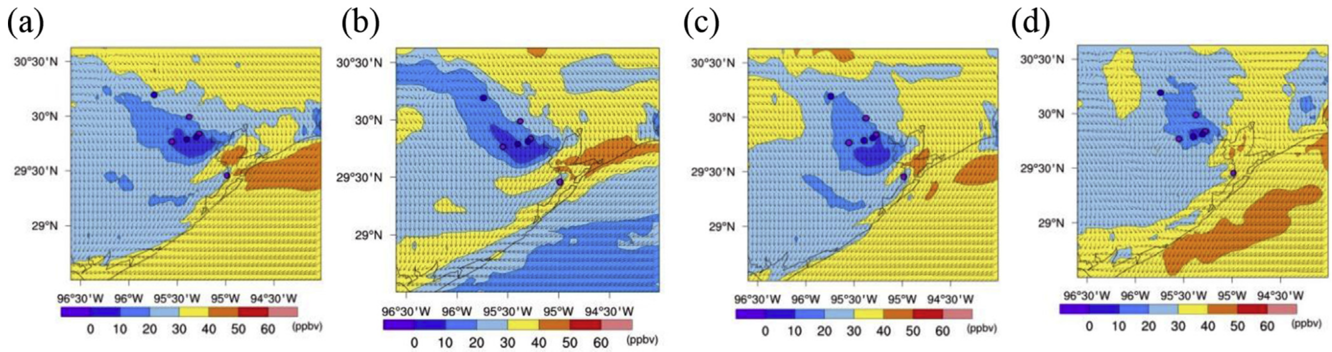

Fig. 6. Spatial distribution of ozone (ppbv) simulated by WRF/Chem and observed by CAMS at 06:00 CDT on October 05, 2006, from experiments with different PBL schemes: (a) YSU, (b) MYJ, (c) ACM2, and (d) QNSE.

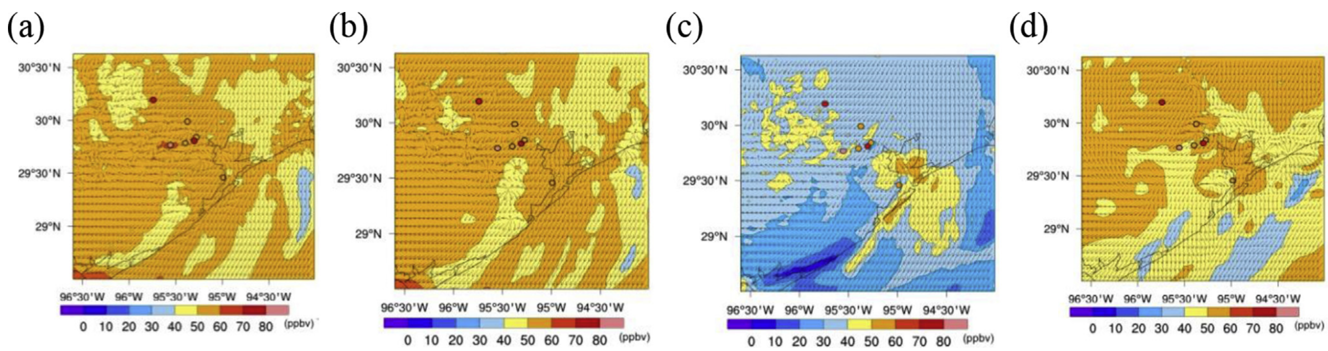

Fig. 7. Spatial distribution of ozone (ppbv) simulated by WRF/Chem and observed by CAMS at 15:00 CDT on October 05, 2006, from experiments with different PBL schemes: (a) YSU, (b) MYJ, (c) ACM2, and (d) QNSE.

deposition and NO titration with limited resupply of O_3-rich air from aloft (e.g. Talbot et al., 2005). Air quality models such as WRF/Chem tend to overestimate ground-level O_3 during the nighttime and this discrepancy is partially attributed to the underestimation of dry deposition (Mao et al., 2006; Chen et al., 2008; Zhang et al., 2009; Lin and McElroy, 2010).

Table S3 in SM displays the statistical analysis of the model result experiments versus observed data for temperature, relative humidity, u–v wind components, and ozone as collected at the two University of Houston sites. The comparison of the modeled wind components at these sites shows higher correlation and smaller bias for the v-component than for the u-component. When

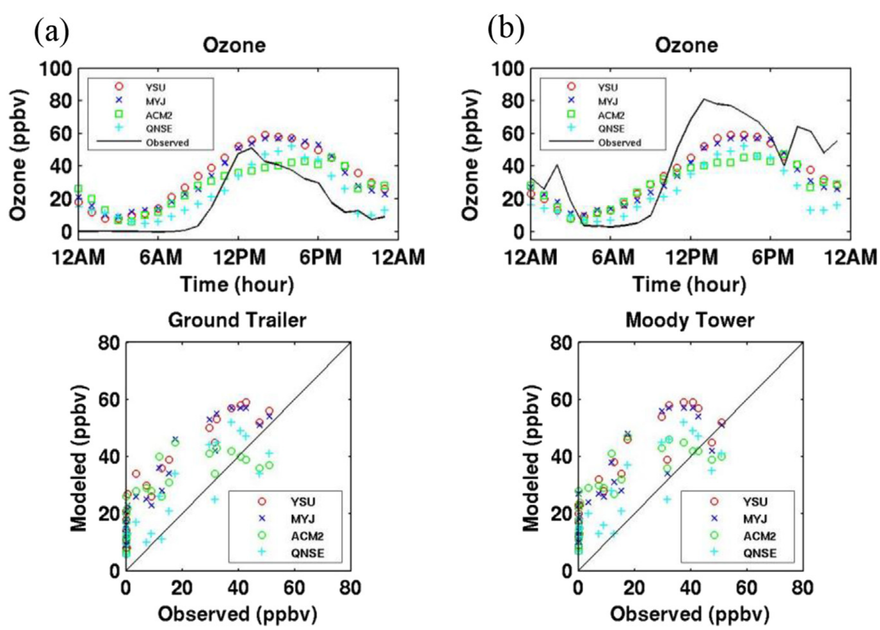

Fig. 8. Simulated ozone time series versus observations at the Ground Trailer (a) and Moody tower (b) on October 05, 2006, and the respective scatter plot below.

comparing the PBL schemes experiments there is no outstanding scheme for this case. The YSU scheme had the highest correlation coefficient, with values of $R > 0.9$, but also shows higher RMSE (18 ppbv) near surface. In the comparison between modeled and observed ozone at the Moody Tower site, i.e. the second model layer, the QSNE scheme yields highest correlation coefficient, with values $R = 0.90$, but also shows higher BIAS (0.80) and RMSE (19 ppbv).

These overestimations of O_3 by the model at night can be observed in almost all comparisons with the CAMS observed data (Fig. S4). The best nighttime model results for O_3 were obtained at the Clinton (C403), and Northwest Harris (C26) stations (Fig. S4c and d, respectively). During the daytime, the Houston East (C1) and Texas City (C620) stations showed the best model results for the surface O_3 (Fig. S4c and d, respectively).

Due to missing NO_x observations at the University of Houston in this period, we conducted a comparison between NO_x simulated by WRF/Chem and observations at CAMS sites (Fig. S5). The simulation of NO_x is a challenge, mainly in cities such as Houston with significant mobile and industrial NO_x emission sources. Overall, WRF/Chem tends to overestimate NO_x, in particular at night under stable boundary layer conditions (Fig. S5a,c,d), e.g. for the C1 and C403 sites (Fig. S5a,c). These two stations are located in the Houston Ship Channel, which is heavily impacted by industrial activities.

These results are similar to that found by Kim et al. (2011), who compared satellite observations with the National Emission Inventory (NEI-2005) NO_x emissions inventory. The authors noticed an overestimation of NO_x in the Houston Ship Channel, while NO_x emissions in the urban Houston area were reasonably represented. In addition, the differences between the WRF/Chem runs are clear, these differences reach up to 100 ppbv at night (Fig. S5f,c) and up to 200 ppbv during daytime (Fig. S5a). These discrepancies in NO_x could lead to differences in O_3 simulated by the model. The same analysis made for UH sites was performed for the CAMS sites. The results are listed in Table S4 in SM. Among the experiments the YSU scheme shows highest R (>0.79) for all stations, and smaller RMSE (<21 ppbv).

3.4. Three-dimension ozone simulation

Figs. 9 and 10 show comparisons of O_3 calculated by WRF/Chem and observed by ozonesonde and tethersonde. Early in the morning (Fig. 9a) the model calculated reasonably well the vertical profile of O_3 as retrieved by the ozonesonde, but there is an overestimation below 800 m agl for all WRF/Chem runs. Fig. 9b presents the results for the ozone profile at 11 CDT. All the WRF/Chem runs underestimate the O_3 profile by a fraction of 30% throughout.

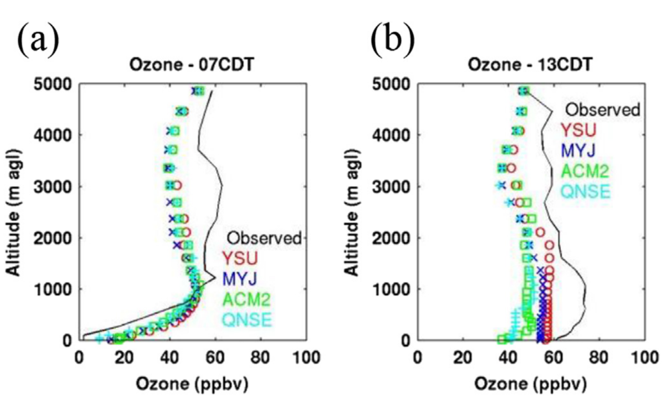

Fig. 9. Simulated vertical profiles of ozone versus ozonesondes at 7 CDT (a) and 13 CDT (b) on October 05, 2006.

Similar results can be observed in the O_3 measurements made by the tethersonde (Fig. 10). The observations at 8:34, and 09:32, (Fig. 10a, b respectively) show that the model captures the values in the first levels of the model (12, 46, 97, 180, 268, 360, 443 m agl), with YSU being the scheme that represents best O_3. During the early afternoon hours, i.e. 12:04 CDT (Fig. 10c) the model did not simulate well the relatively fast increase of O_3 from 60 ppbv at 12:04 CDT up to approximately 80 ppbv at 18:31 CDT (Fig. 10d).

To analyze the model biases in the vertical distribution of O_3, we conducted a comparison between CO, NO_x, HCHO, and SO_2 calculated by the model and observed aboard the Aztec aircraft (Figs. 11 and 12, and in SM Figs. S6, S7). To analyze the accuracy of vertical mixing in the model, CO observed by the Aztec aircraft was compared with the WRF/Chem model results. Carbon monoxide is a very slow reacting trace gas and is an important tropospheric pollutant. Fig. 11a, b presents vertical profiles of CO calculated by the model and observed by the Aztec aircraft. There is an accumulation of CO close to the surface simulated by MYJ, ACM2, and QNSE schemes due to both suppressed mixing and high emissions at the same time. In the second (Fig. 11a) the simulated CO values are in relatively agreement with the observed values, but near the surface (below 200 m agl) there is an overestimation of the model. In the spins 4 (Fig. 11b) the experiments show relatively good comparison with the observed values above 1000 m agl, but underestimate observed values in the layers between 200 and 1000 m agl, and overestimate again below 200 m agl for QNSE and ACM2 scheme. The same statistical analysis made for previous data was performed for the Aztec aircraft measurements. The results are listed in Table S5 in SM. Among the experiments the YSU scheme shows highest R for CO in all spins.

Nitrogen oxides (Fig. 12) are relatively well mixed in the boundary layer based on YSU scheme, which showed the best agreement with the measurements. There is an accumulation of NO_x near the ground simulated by MYJ, ACM2, and QNSE schemes indicating that there is a lack of vertical mixing in the boundary layer, in particular during daytime. Formaldehyde is important as a tracer for HO_x production (Fried et al., 1997). HCHO is fairly short-lived ($\tau \approx 3$ h) and is removed from the atmosphere primarily by reaction with OH and by photolysis (Hak et al., 2005). Each of these processes produce HO_2 (Anderson et al. 1996; Calvert et al., 2000) and result in a net production of O_3 in the presence of NO_x. Making accurate estimates of these species is crucial to atmospheric modeling on both local and global scales. Note that there is no observational data for NO_x in spin number 1 available (denoted as "n/a"). Fig. S6 presents vertical profiles of HCHO calculated by the model and observed by the Aztec aircraft. In the first spin (Fig. S6a) the calculated HCHO values largely agree with the observed values near the surface, but there is an underestimation of the model between 200 and 1000 m. In the spins 5 (Fig. S6e), the experiments show the similar behavior as NO_x, where the YSU scheme presents the finest vertical mixing among the experiments for this particular case. However, there is a notorious underestimation of the HCHO values calculated by the model when compared with observations below 2000 m agl. These differences range from approximately 1, 2, and 3 ppbv for spin 3, 4 and 5, respectively. Sulfur dioxide (Fig. S7) presented same behavior as CO with values in relatively agreement with the observed values, but also showed an accumulation of SO_2 close to the surface. Among the experiments the YSU scheme presents the highest R values in almost all spins for NO_x, and QNSE shows the highest R values for HCHO and SO_2. The statistical analysis for O_3 shows high R values (>0.69) for spins 1,2,3, and 5; spin number 4 presents poor correlation between simulated and observed values (Table S5). Although the QNSE scheme shows higher R values than the YSU scheme for O_3 in spins 1 and 2, there is evidence that the YSU scheme displays high R values more

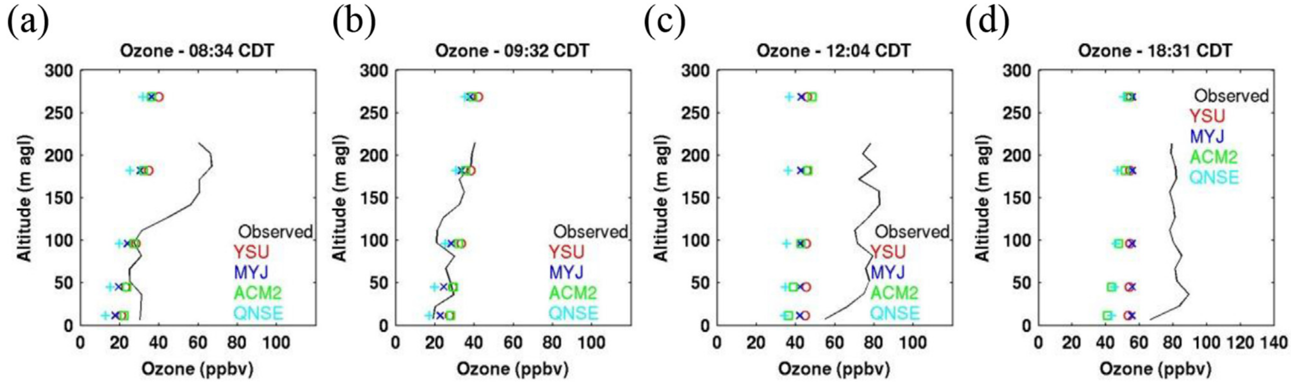

Fig. 10. Simulated vertical profiles of ozone versus tethersonde ozone data at 08:34 CDT (a), 09:32 CDT (b), 12:04 CDT (c), and 18:31 CDT (d) on October 5, 2006.

frequently than other schemes. Also, there is a chance that the YSU scheme may fail under specific conditions for O_3 (e.g. spin 4) albeit less often than the other PBL schemes (Table S5).

The distinct way turbulent diffusion is represented in the different PBL schemes may provide an explanation for the huge discrepancies between experiments. In the current WRF/Chem model, the turbulent diffusion is not calculated in the ACM2 scheme and a small vertical diffusion coefficient (1.0×10^{-6} m^2 s^{-1}) is used for the vertical mixing of chemical species (Hu et al., 2012). In the MYJ and YSU schemes, the turbulent diffusion coefficient (~10^2 m^2 s^{-1} in the daytime boundary layer) is used for vertical mixing of chemical species. As there are significant differences in the vertical mixing due to distinct turbulent exchange coefficients, this will have an impact on the vertical transport of surface CO, NO_x, HCHO and SO_2.

The results illustrate that the MYJ, ACM2, and QNSE in WRF/Chem do not properly simulate the vertical mixing of chemical species. This may explain some of the differences between the surface O_3 predicted by WRF/Chem coupled with different PBL schemes, which are also reported in Yerramilli et al. (2010). Thus, the current WRF/Chem model needs revision to estimate the vertical transport of chemical species in a more realistic way. Among the different experiments the YSU scheme simulates best the vertical profile of CO, NO_x, and SO_2. This could be the reason why this scheme also better presents O_3. Therefore, one important conclusion of this study is that models such as WRF/Chem require improved numerical algorithms to properly account for the nocturnal vertical transport of O_3 in the residual layer of the PBL, and also specific adjustments to better represent highly complex air quality conditions such as present in Houston.

4. Conclusions

In this study, we performed a sensitivity analysis study of WRF/Chem employing different PBL schemes and pointed to some potential impacts on surface ozone concentrations in the Houston metropolitan area. As a case study, we chose the 24-h period of

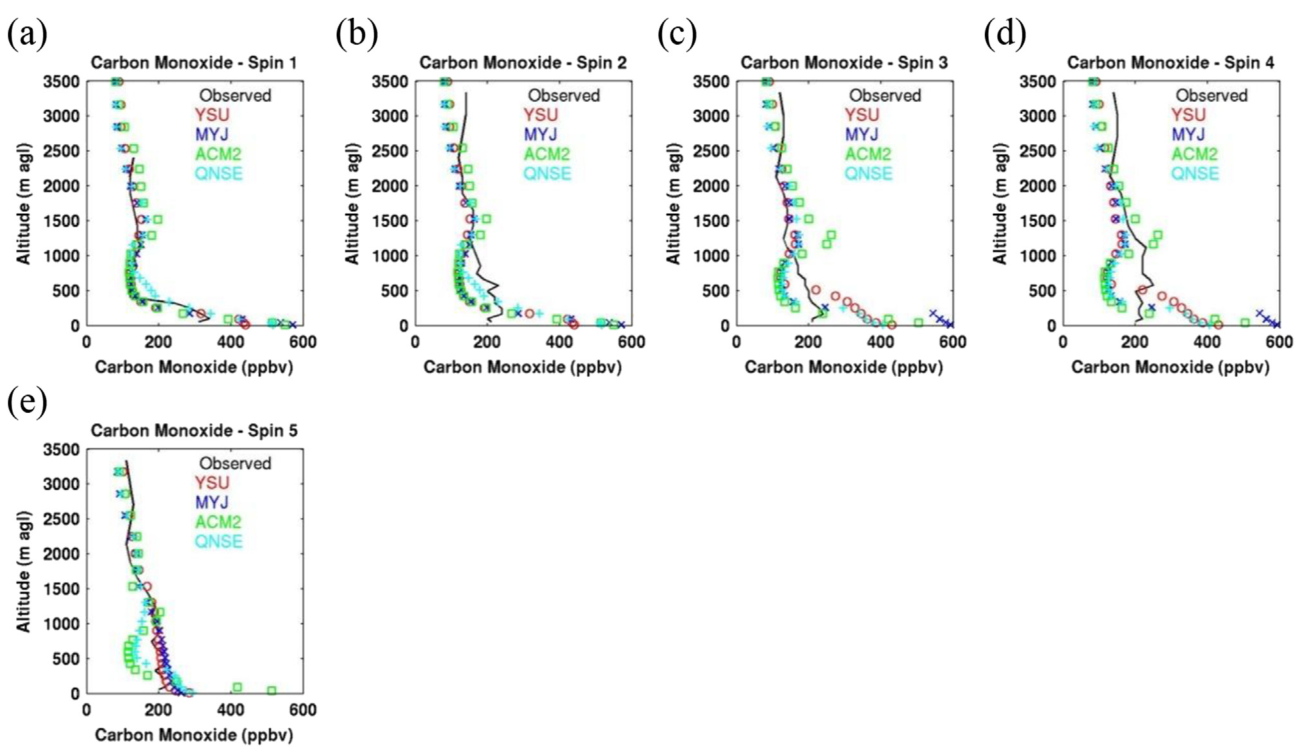

Fig. 11. Simulated vertical profiles of CO versus CO measurements aboard the Aztec aircraft for 5 spins made on October 5, 2006,: spin 1 from 10:16 to 11:09 a.m. CDT (a); spin 2 from 11:10 to 11:29 a.m. CDT (b); spin 3 from 11:36 to 12:20 a.m. CDT (c); spin 4 from 12:21 to 12:57 a.m. CDT (d); and spin 5 from 12:58 a.m. to 01:40 p.m. CDT (e).

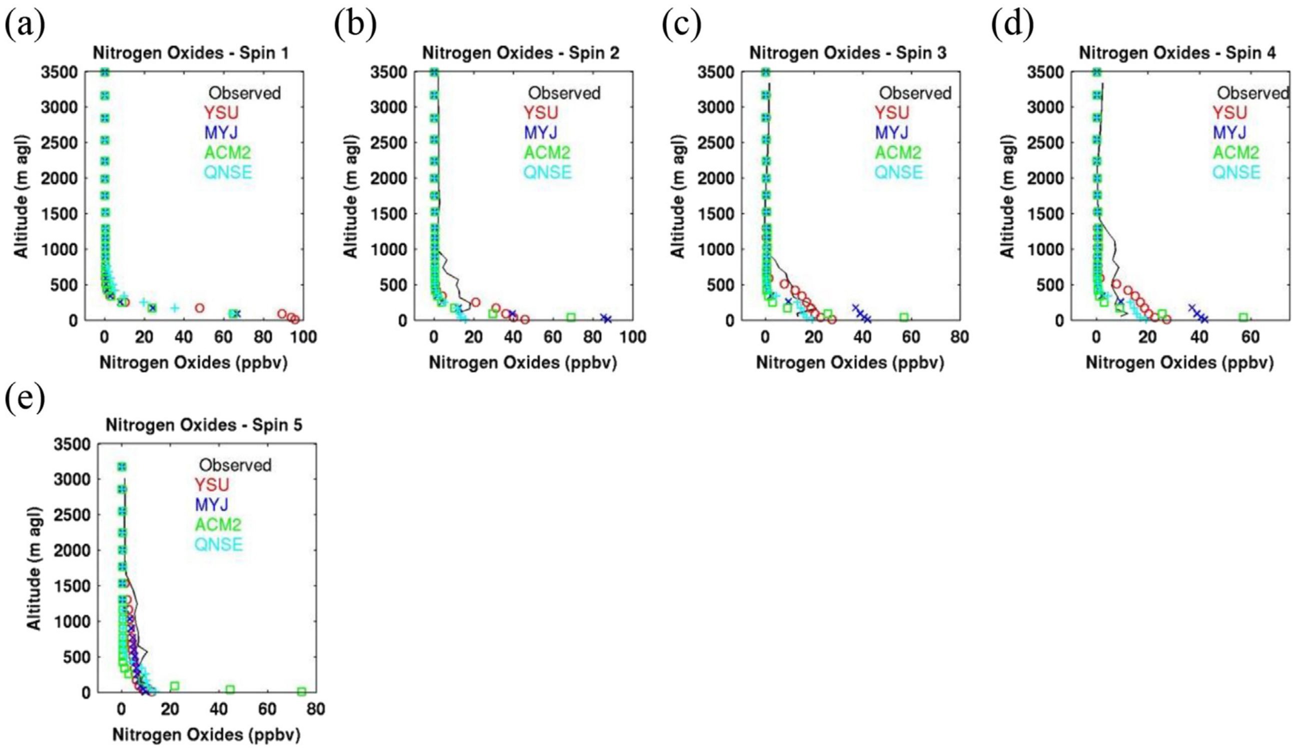

Fig. 12. Simulated vertical profiles of NO_x versus NO_x measurements aboard the Aztec aircraft for 5 spins made on October 5, 2006: spin 1 from 10:16 to 11:09 a.m. CDT (a); spin 2 from 11:10 to 11:29 a.m. CDT (b); spin 3 from 11:36 to 12:20 a.m. CDT (c); spin 4 from 12:21 to 12:57 a.m. CDT (d); and spin 5 from 12:58 a.m. to 01:40 p.m. CDT (e).

October 5, 2006. Weather conditions were characterized by a pre-frontal passage, which resulted in light northern winds, high temperatures, and high humidity.

In a first step, we made an evaluation of some simulated meteorological variables using observational data from the VME project. The results indicated that the model simulates well the ambient temperature, potential temperature, water vapor mixing ratio, and relative humidity. These variables show high correlation coefficients (0.9) and low biases not only in surface but also in the vertical profiles. While the model provided good results in calculating wind components in the first model level, the vertical variations of the wind are not well simulated. The representation of the surface variables still has large uncertainties, especially under stable conditions. There is no particularly well-suited algorithm.

In a second step, we examined the sensitivity of ozone concentration in the WRF/Chem model to different PBL schemes. Model evaluations showed that, during the daytime, WRF/Chem simulated reasonably well maximum ground-level O_3 at most stations, including the CAMS sites, during the Vertical Mixing Experiment. On the other hand, during the nighttime, simulated O_3 levels compared poorly with measurements and largely overestimated the observed single digit values of O_3 at some stations. Poor performance was possible due to underestimation of dry deposition velocity and overestimation of NO titration of ozone in the model. The result from the PBL experiment shows that the YSU scheme improves performance in specific subsets of observations. It may be the best of these 4 PBL parameterizations to represent the vertical mixing of O_3 precursors in this particular case, and this result is highlighted when WRF/Chem results are compared with observed values of CO, NO_x, and HCHO. Further investigation is necessary to arrive at a final conclusion. The comparison of vertical profiles showed that the model captures well the O_3 profile in the first hours of the morning, but in the afternoon the model underestimated the values of O_3.

Acknowledgments

We acknowledged the financial support provided by CAPES (Grant No.: 5837-10-3). We gratefully acknowledge financial and logistic support of the Houston Advanced Research Center (HARC) (Grant No.: H78 Modification C (582-4-65587)), the Texas Commission on Environmental Quality (TCEQ) (Grant No.: 582-5-64594-01), and the University of Houston to obtain the data within the TRAMP study.

Appendix A. Supplementary material

Supplementary material related to this article can be found at http://dx.doi.org/10.1016/j.atmosenv.2014.07.013.

References

Anderson, L.G., Lanning, J.A., Barrell, R., Miyagishima, J., Jones, R., Wolfe, P., 1996. Sources and sinks of formaldehyde and acetaldehyde: an analysis of Denver's ambient concentration data. Atmos. Environ. 30, 2113–2123.

Blackadar, A.K., January 1978. Modeling pollutant transfer during daytime convection. In: American Meteorology Society, 4th Symposium on Atmospheric Turbulence, Diffusion, and Air Pollution, Reno/NV.

Borge, R., Alexandrov, V., del Vas, J.J., Lumbreras, J., Rodriguez, E., 2008. A comprehensive sensitivity analysis of the WRF model for air quality applications over the Iberian Peninsula. Atmos. Environ. 42 (37), 8560–8574. http://dx.doi.org/10.1016/j.atmosenv.2008.08.032.

Calvert, J.G., Atkinson, R., Kerr, J.A., Madronich, S., Moortgat, G.K., Wallington, T., Yarwood, G., 2000. The Mechanisms of Atmospheric Oxidation of the Alkenes. Oxford University Press, Oxford.

Chen, J., Vaughan, J., Avise, J., O'Neill, S., Lamb, B., 2008. Enhancement and evaluation of the AIRPACT ozone and PM2.5 forecast system for the Pacific Northwest. J. Geophys. Res. 113, D14305. http://dx.doi.org/10.1029/2007JD009554.

Cheng, Y., Steenburgh, J., 2005. Evaluation of surface sensible weather forecasts by the WRF and the eta models over the Western United States. Weather Forecast. 20, 812–821. http://dx.doi.org/10.1175/WAF885.1.

Day, B.M., Rappenglück, B., Clements, C.B., Tucker, S.C., Brewer, W.A., 2010. Nocturnal boundary layer characteristics and land breeze development in

Houston, Texas, during TexAQS-II. Atmos. Environ. 44, 4014–4023. http://dx.doi.org/10.1016/j.atmosenv.2009.01.031.
Fried, A., Sewell, S., Henry, B., Wert, B., Gilpin, T., Drummond, J., 1997. Tunable diode laser absorption spectrometer for ground-based measurements of formaldehyde. J. Geophys. Res. 102, 6283. http://dx.doi.org/10.1029/96JD01580.
Gilliam, R.C., Pleim, J.E., 2010. Performance assessment of new land surface and planetary boundary layer physics in the WRF-ARW. J. Appl. Meteorol. Climatol. 49 (4), 760–774. http://dx.doi.org/10.1175/2009jamc2126.1.
Grell, G.A., Peckham, S.E., Schmitz, R., Mckeen, S.A., Wilczak, J., Eder, B., 2005. Fully coupled "online" chemistry within the WRF model. Atmos. Environ. 39, 6957–6975.
Ha, K.-J., Mahrt, L., 2001. Simple inclusion of z-less turbulence within and above the modeled nocturnal boundary layer. Mon. Weather Rev. 129, 2136–2143.
Hak, C., Pundt, I., Trick, S., Kern, C., Platt, U., Dommen, J., Ordóñez, C., Prévôt, A.S.H., Junkermann, W., Astorga-Lloréns, C., Larsen, B.R., Mellqvist, J., Strandberg, A., Yu, Y., Galle, B., Kleffmann, J., Lörzer, J.C., Braathen, G.O., Volkamer, R., 2005. Intercomparison of four different in-situ techniques for ambient formaldehyde measurements in urban air. Atmos. Chem. Phys. 5, 2881–2900.
Holt, T., Raman, S., 1988. A review and comparative evaluation of multilevel boundary layer parameterizations for first-order and turbulent kinetic energy closure schemes. Rev. Geophys. 26, 761–780.
Hu, X., Doughtya, D., Sanchez, K., Joseph, E., Fuentes, J., 2012. Ozone variability in the atmospheric boundary layer in Maryland and its implications for vertical transport model. Atmos. Environ. 46, 354–364. http://dx.doi.org/10.1016/j.atmosenv.2011.09.054.
Hu, X., Nielsen-Gammon, J., Zhang, F., 2010. Evaluation of three planetary boundary layer schemes in the WRF model. J. Appl. Meteorol. Climatol. 49, 1831–1844. http://dx.doi.org/10.1175/2010JAMC2432.1.
Hu, X., Klein, P.M., Xue, M., 2013. Evaluation of the updated YSU planetary boundary layer scheme within WRF for wind resource and air quality assessments. J. Geophys. Res. Atmos. 118, 10,490–10,505. http://dx.doi.org/10.1002/jgrd.50823.
Jankov, I., Schultz, P.J., Anderson, C.J., Koch, S.E., 2007. The impact of different physical parameterizations and their interactions on cold season QPF in the American River Basin. J. Hydrometeorol. 8 (5), 1141–1151. http://dx.doi.org/10.1175/Jhm630.1.
Kim, S.-W., McKeen, S., Frost, G., Lee, S., Trainer, M., Richter, A., Angevine, W., Atlas, E., Bianco, L., Boersma, K., Brioude, J., Burrows, J., Gouw, J., Fried, A., Gleason, J., Hilboll, A., Mellqvist, Peischl, J., Richter, D., Rivera, C., Ryerson, T., Lintel Hekkert, S., Walega, J., Warneke, C., Weibring, P., Williams, E., 2011. Evaluation of NO_x and highly reactive VOC emission inventories in the Texas and their implications for ozone plume simulations during the Texas Air Quality Study 2006. Atmos. Chem. Phys. 11, 11361–11386. http://dx.doi.org/10.5194/acp-11-11361-2011.
Kolling, J., Pleim, J., Jeffries, H., Vizuete, W., 2013. A multisensor evaluation of the asymmetric convection model, version 2, in Southeast Texas. J. Air Waste Man. Assoc. 63 (1), 41–53. http://dx.doi.org/10.1080/10962247.2012.732019.
Lefer, B., Rappenglueck, B., 2010. The TexAQS-II radical and aerosol measurement project (TRAMP) preface. Atmos. Environ. 44 (33), 3997–4004.
Lin, J.T., McElroy, M.B., 2010. Impacts of boundary layer mixing on pollutant vertical profiles in the lower troposphere: implications to satellite remote sensing. Atmos. Environ. 44 (14), 1726–1739.
Madronich, S., 1987. Photodissociation in the atmosphere, 1, actinic flux and the effects of ground reflections and clouds. J. Geophys. Res. 92, 9740–9752.
Mao, Q., Gautney, L.L., Cook, T.M., Jacobs, M.E., Smith, S.N., Kelsoe, J.J., 2006. Numerical experiments on MM5-CMAQ sensitivity to various PBL schemes. Atmos. Environ. 40, 3092–3110.
Misenis, C., Hu, X., Krishnan, S., Zhang, Y., Fast, J.D. Sensitivity of WRF/CHEM predictions to meteorological schemes. In: 86th Annual AMS Conference and the 14th Joint Conference on the Applications of Air Pollution Meteorology with the A&WMA, Atlanta/GA, USA, January-February 2006.
Mohan, M., Bhati, S., 2011. Analysis of WRF model performance over subtropical region of Delhi. India Adv. Meteorol. http://dx.doi.org/10.1155/2011/621235.
Ngan, F., Kim, H., Lee, P., Al-Wali, K., Dornblaser, B., 2013. A study of nocturnal surface wind speed overprediction by the WRF-ARW model in Southeastern Texas. J. Appl. Meteorol. Climatol. 52, 2638–2653. http://dx.doi.org/10.1175/JAMC-D-13-060.1.
Olaguer, E.P., Rappenglück, B., Lefer, B., Stutz, J., Dibb, J., Griffin, R., Brune, B., Shauck, M., Buhr, M., Jeffries, H., Vizuete, W., Pinto, J., 2009. Deciphering the role of radical sources during the second Texas air quality study. J. Air Waste Man. Assoc. 59, 1258–1277.
Rappenglück, B., Perna, R., Zhong, S., Morris, G.A., 2008. An analysis of the vertical structure of the atmosphere and the upper-level meteorology and their impact on surface ozone levels in Houston/TX. J. Geophys. Res. 113, D17315. http://dx.doi.org/10.1029/2007JD009745.
Roux, G., Liu, Y., Monache, L.D., Sheu, R.Y., Warner, T.T., June 2009. Verification of high resolution WRF-RTFDDA surface forecasts over mountains and plains. In: 10th WRF Users' Workshop, Boulder, Colorado, USA.
Skamarock, W.C., Klemp, J.B., Dudhia, J., Gill, D.O., Barker, D.M., Duda, M.G., Huang, H.-Y., Wang, W., Powers, J.G., 2008. A Description of the Advanced Research WRF Version 3. NCAR Tech. Note NCAR/TN-475STR, p. 113.
Stull, R.B., 1988. An Introduction to Boundary Layer Meteorology. Kluwer, The Netherlands, p. 666.
Stull, R.B., Driedonks, A.G.M., 1987. Applications of the transilient turbulence parameterization to atmospheric boundary-layer simulations. Bound. Layer Met. 40, 209–239.
Talbot, R., Mao, H., Sive, B., 2005. Diurnal characteristics of surface level O_3 and other important trace gases in New England. J. Geophys. Res. 110, D09307. http://dx.doi.org/10.1029/2004JD005449.
Tang, W., Cohan, D., Morris, G., Byun, D., Luke, W., 2011. Influence of vertical mixing uncertaninties on ozone simulation in CMAQ. Atmos. Environ. 45, 2898–2909. http://dx.doi.org/10.1016/j.atmosenv.2011.01.057.
U.S. Environmental Protection Agency (U.S. EPA), 2008. Regulatory Impact Analysis, 2008 National Ambient Air Qualty Standards for Ground Level Ozone, Chapter 6. Office of Air Quality Planning and Standards, Research Triangle Park, NC. March. Available at: http://www.epa.gov/ttn/ecas/regdata/RIAs/6ozoneriachapter6.pdf.
Wesley, M.L., 1989. Parameterization of surface resistance to gaseous dry deposition in regional numerical models. Atmos. Environ. 16, 1293–1304.
Wilmot, C.-S., Rappenglück, B., Li, X., 2014. MM5 v3.6.1 and WRF v3.2.1 model comparison of standard and surface energy variables in the development of the planetary boundary layer. Geosci. Model Dev. Discuss. 7, 1–39. http://dx.doi.org/10.5194/gmdd-7-1-2014.
Xie, B., Hunt, J.C.R., Carruthers, D.J., Fung, J.C.H., Barlow, J.F., 2013. Structure of the planetary boundary layer over Southeast England: modeling and measurements. J. Geophys. Res. Atmos. 118, 7799–7818. http://dx.doi.org/10.1002/jgrd.50621.
Yerramilli, A., Challa, V., Dodla, V., Dasari, H., Young, J., Patrick, C., Baham, J., Hughes, R., Hardy, M., Swanier, S., 2010. Simulation of surface ozone pollution in the central Gulf Coast region using WRF/Chem model: sensitivity to PBL and land surface physics. Adv. Meteorol. 2010, 1–24. http://dx.doi.org/10.115/2010/319138.
Yver, C.E., Graven, H.D., Lucas, D.D., Cameron-Smith, P.J., Keeling, R.F., Weiss, R.F., 2013. Evaluating transport in the WRF model along the California coast. Atmos. Chem. Phys. 13 (4), 1837–1852. http://dx.doi.org/10.5194/acp-13-1837-2013.
Zhang, Y., Dubey, M.K., Olsen, S.C., Zheng, J., Zhang, R., 2009. Comparisons of WRF/Chem simulations in Mexico City with ground-based RAMA measurements during the 2006-MILAGRO. Atmos. Chem. Phys. 9, 3777–3798.